Structural and magnetic properties of $SmCo_5$+30%α-Fe exchange coupled nanocomposites obtained by mechanical milling

R. HIRIAN[a], O. ISNARD[b, c], V. POP[a,*]
[a]*Faculty of Physics, Babeş-Bolyai University, Cluj-Napoca, RO-400084 Romania*
[b]*University Grenoble Alpes, Institut NÉEL, 25 rue des martyrs, F-38042 Grenoble, France*
[c]*CNRS, Institut NÉEL, 25 rue des martyrs, F-38042 Grenoble, France*

The magnetic and structural properties of $SmCo_5$+30%Fe magnetic nanocomposites obtained through mechanical milling are investigated by DSC, TGA, XRD and magnetic measurements. It is shown that above 923 K (650 °C) the hard and soft magnetic phases react to form $Sm_2(Co\text{-}Fe)_{17}$ as the hard magnetic phase and Fe-Co as the soft magnetic phase which leads to a significant loss of anisotropy. The difference in magnetic behavior between the nanocomposites exposed to high temperatures (up to 1323 K, 1050 °C) and those annealed at 873 K (600 °C) was analyzed.

(Received March 1, 2019; accepted October 9, 2019)

Keywords: Nanocomposite, Spring magnet, Phase transition, Exchange coupling, Magnetic properties

1. Introduction

High performance rare-earth based permanent magnets are ubiquitous in the modern world [1-3]. However, due to the geographic distribution of lanthanide deposits, significant market instability (still in recent memory) and the significant ecologic impact of rare-earth mining and processing [4], current research is focused on reducing the dependence on lanthanides for permanent magnet applications. One promising avenue is the spring magnet [5], a nanocomposite material in which a hard magnetic phase is used to stiffen the high magnetization of a soft magnetic phase. The draw of spring magnets comes chiefly from the predicted theoretical energy product of more than 1 MJ/m^3 [6], nearly double that of the current generation of high performance permanent magnets. Moreover, besides the high energy product, spring magnets also possess improved thermal stability [7] enhanced corrosion resistance [8] and surface passivation [9] compared to the current generation of rare-earth based high performance permanent magnet materials. Attempts to produce such a material were made using a plethora of synthesis techniques: melt-spinning [10], mechanical milling [11], sono-chemical synthesis [12], bulk injection casting [13], suction casting [14], hot deformation [15], thin films [16] etc. the latter being the most successful attempt, with obtained energy products of over 400 kJ/m^3.

Following previous work on $SmCo_5$+20wt%α-Fe nanocomposite powders produced through mechanical milling [17-19], we have decided on the one hand to revisit the feasibility of increasing the α-Fe content [20] of the materials hoping to obtain an increase in the energy product, while also investigating the high temperature behavior of $SmCo_5$/α-Fe nanocomposites.

2. Experimental details

The $SmCo_5$ ingot was produced (from pure elements) by induction melting and subsequent annealing at 950 °C for 72 h under purified Ar atmosphere. The starting powder was made by mixing the crushed and sieved $SmCo_5$ alloy (particle size < 500 μm) with 30 wt% commercial NC 100.24 Fe powder (particles size < 100 μm). The mixture was dry milled (MM), in a Fritsch Pulverisette 4 planetary mill, under Ar gas, for 6 hours using 26 balls with Ø = 10 mm diameter. The milling vials and balls are made of 440C hardened steel. The ratio between the rotation speed of the disk and the rotation speed of the vials was Ω/ω = -333 /900 with a ball to powder weight ratio of 10:1. The milled powder was then wrapped in tantalum foil, sealed in a quartz tube under Ar atmosphere and annealed. All powder manipulation was done under inert Ar atmosphere inside a glove box. The structure and microstructure of the annealed samples were investigated by X-ray diffraction (XRD) using a Bruker D8 Advance diffractometer equipped with a Cu-Kα radiation and Bragg–Brentano focusing geometry. Differential scanning Calorimetry (DSC) and thermogravimetric analysis (TGA) measurements were performed on a TA-Instruments Q600 STA, in the temperature range of 300-950 K. Thermo-magnetic measurements were done on a Faraday type magnetic balance in the temperature range of 300-1323 K. The demagnetization curves were recorded on a Cryogenics vibrating sample magnetometer (VSM), at room temperature and applied fields of up to 10 T. Because the powders were blocked in epoxy resin for these measurements, the calculations for the internal field (H_{int})

were done in the approximation of dilute magnetic substances containing spherical particles [21].

3. Results and discussions

The DSC measurements on $SmCo_5$+30%Fe nanocomposite powders are shown in Fig. 1. Two large exothermic peaks are identified at 780 K and 920 K. The peak at 780 K can be associated with the recrystallization temperature of both the α-Fe and $SmCo_5$ phases, while the peak at 920 K can be associated with the formation of the $Sm_2(Co_{1-x}Fe_x)_{17}$ phase. The broad feature, which starts at 500 K, is associated with strain and defect removal from the milled powder.

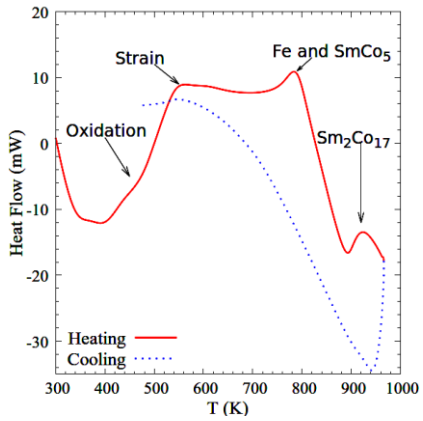

Fig. 1. DSC curves for 6 h MM $SmCo_5$+30%Fe magnetic nanocomposites

A small kink at 450-500 K denotes the start of oxidation, a fact confirmed from the TGA measurements, Fig. 2. The sample mass begins to increase at the noted temperature due to the formation of samarium oxides. Along with the formation of Sm-oxides, free Co is produced.

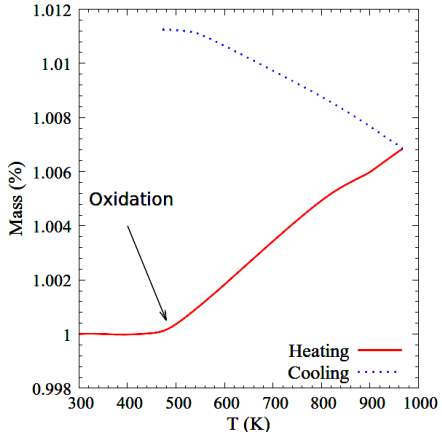

Fig. 2. TGA measurements for 6 h MM $SmCo_5$+30%Fe magnetic nanocomposites

The thermo-magnetic measurements support the conclusions drawn from the DSC measurements. Figure 3, shows the presence of two critical temperatures for 6 h MM $SmCo_5$+30%Fe nanocomposites. The first one at 1076 K is associated with the Curie temperature of $Sm_2(Co_{1-x}Fe_x)_{17}$ for x ≈ 0.4 [22]. Furthermore, the lower value of T_c=1020 K for $SmCo_5$ [22] is absent, therefore we must conclude that after heating above 920 K the entirety of the $SmCo_5$ phase has transitioned into the $Sm(Co_{1-x}Fe_x)_{17}$ phase. The second transition is likely due to the Fe-Co soft magnetic phase, as it transitions from the BCC (Im-3m) low temperature structure into the non-magnetic FCC (Fm-3m) one [23] on the heating curve (the reverse is true for the cooling curve). The phase transition could also account for the large transition temperature difference seen between the heating and cooling curves (ΔT = 40 K). The fact that the magnetization does not reach zero value after the second critical temperature may indicate the presence of the α-Co phase. Moreover, the decreasing magnetization observed on the cooling curve in this region suggests that the Co, produced through the aforementioned oxidation process, is absorbed into the Fe-Co alloy becoming non-magnetic in this temperature region. However, the low residual magnetization signal shows that the pure Co phase content is very low. It is assumed that the Fe-Co alloy [17] is formed from the loose Co and the initial soft magnetic phase (Fe). The obtained Curie temperature for the $Fe_{1-x}Co_x$ alloy indicates an x of around 0.3; however the exact composition has proven difficult to pin down. The relatively high concentration of Co in the soft magnetic phase, though surprising at first glance, becomes easier to accept taking into account the fact that a large amount of the initial Fe is necessary for the formation of the doped $Sm_2(Co_{1-x}Fe_x)_{17}$. For x ≈ 0.4 doping of the hard magnetic phase, there are approximately seven Fe atoms for every ten Co atoms, a calculated Fe content of 29.6 wt%/f.u. for $Sm_2(Co_{1-x}Fe_x)_{17}$.

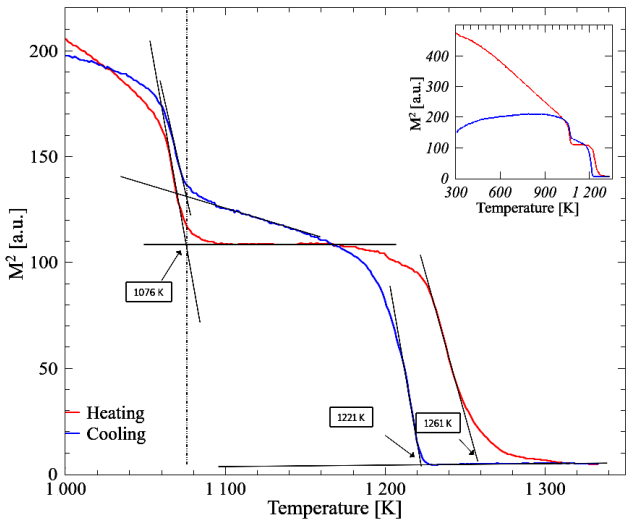

Fig. 3. Temperature dependence of the square of the magnetization for $SmCo_5$+30%Fe magnetic nanocomposites. Full temperature range of measurement is given in inset

In our previous work on $SmCo_5$+30%Fe nanocomposite [20], annealing around 923 K (650 °C) for 30 minutes has proven efficient for the recrystallization of

the hard magnetic phase which was severely damaged during the milling process, while also limiting the growth of the soft magnetic phase crystallite. However given that this annealing temperature coincides with the recrystallization temperature of Sm_2Co_{17}, we have decided to lower the annealing temperature to 873 K (600 °C), in order to avoid the formation of the 2:17 phase.

XRD patterns for the $SmCo_5$+30%Fe sample annealed at 873 K (600 °C) for 30 min and for the sample which was measured in the thermo-magnetic balance up to 1323 K (labeled HT) are shown in Fig. 4 along with the calculated patterns for their constituent phases. For the 873 K annealed sample the majority phases are $SmCo_5$ and Fe, which is reasonable as annealing took place below the temperature of the exothermic peak attributed to the formation of the 2:17 phase. However due to the moderate signal to noise ratio the presence of such a phase cannot be excluded, as it could have been formed during the milling process. The sample which was measured in the thermo-magnetic balance shows the presence of the 2:17 rhombohedral structure along with Sm oxides and a Fe-Co alloy. The lattice parameters for the $Sm_2(Co_{1-x}Fe_x)_{17}$ were estimated as a =8.46 Å and c =12.39 Å which again indicate that the value of x is around 0.4 [22]. The average crystallite sizes for the soft magnetic phase were also estimated through XRD using the Scherrer method [24] yielding approximately 10-13 nm for the annealed sample and 100 nm for the HT sample.

Demagnetization curves presented in Fig. 5 show that annealing at 600 °C for 30 min produces samples with a fair degree of interphase exchange coupling. This sample possesses a $\mu_0 H_c$=0.39 T and M_r=90 Am^2/Kg (an increase of 10% and 17% respectively, compared to our previous work [20]) and an M_r/M_s ratio of 0.6. When compared with $SmCo_5$+20%Fe nanocomposites, the samples annealed at 873 K show a 10% increase in remanence and a 60 % decrease in coercivity [19]. Moreover, the calculated energy product for the annealed sample is only 63 KJ/m^3, 40% lower than that of the samples made with 20%Fe.

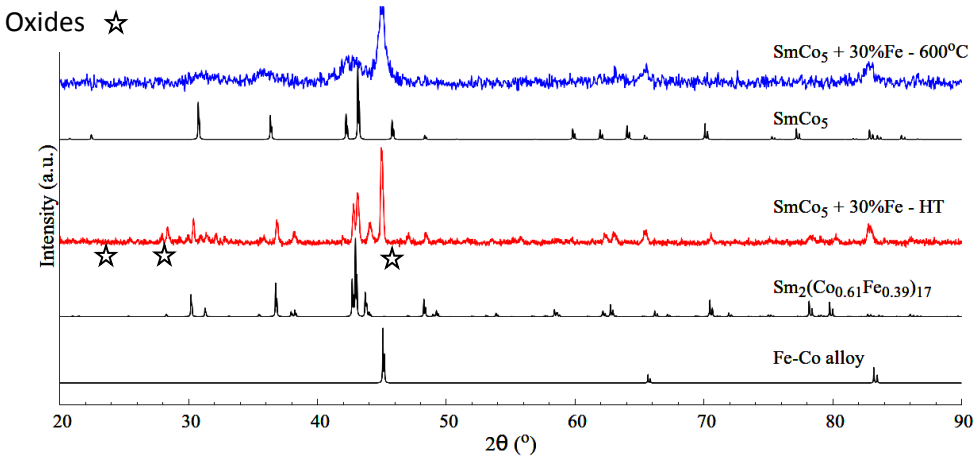

Fig. 4. XRD patterns for 6 h MM $SmCo_5$+30%Fe magnetic nanocomposites along with calculated reference patterns for the constituent phases. For clarity, the Sm_2O_3 pattern was not plotted; however some of the significant peaks were marked by stars

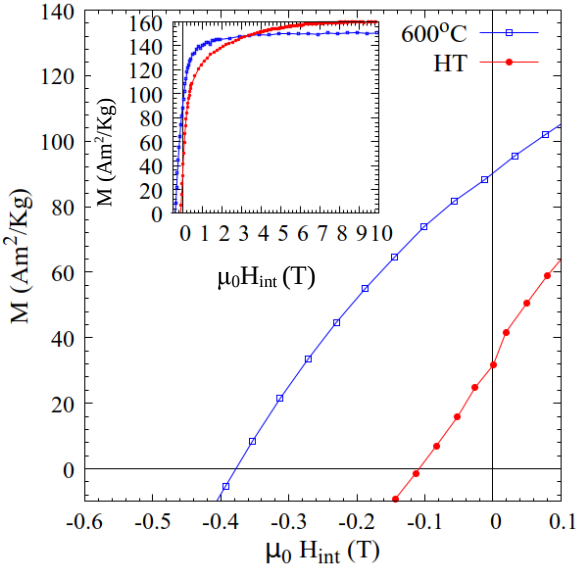

Fig. 5. Demagnetization curves at 300 K for $SmCo_5$+30%Fe magnetic nanocomposites

On the other hand the large Fe sizes recorded for the HT sample (which was heated to 1323 K) lead to a significant reduction in magnetic performance, with a fourfold reduction in H_c, and a threefold reduction in M_r; the M_r/M_s ratio for this samples is only 0.2 while the energy product is a measly 7 KJ/m^3. The *dM/dH vs. H* plots, Fig. 6, paint a more detailed picture, where the large peak centered on 0.4 T for the 873 K annealed sample shows that the majority of reversal processes take place at relatively high field. However the broadness of the peak also means that a significant number of domain reversal events also take place at fields around 0 T. In the case of the HT sample we see a two phase behavior where most reversal processes take place at fields around 0 T (note the very intense peak) while the rest are centered around 0.25 T. The difference in magnetic behavior is in large part due to the difference in Fe crystallite sizes but also due to the fact that the hard magnetic phase changes from $SmCo_5$ to $Sm_2(Co_{0.6}Fe_{0.4})_{17}$ which has a much lower anisotropy (K_1), one order of magnitude lower than $SmCo_5$ and 30-35%

lower than Sm_2Co_{17} [22], making the large Fe inclusions even harder to pin.

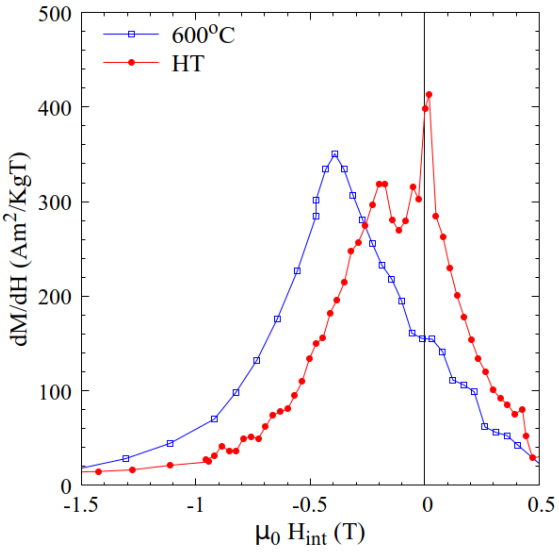

Fig. 6. dM/dH vs H plots at 300 K for $SmCo_5$+30%Fe magnetic nanocomposites

4. Conclusions

The magnetic and structural properties of $SmCo_5$+30%Fe magnetic nanocomposites obtained through mechanical milling were investigated by DSC, TGA, XRD and magnetic measurements.

Annealing at 873 K (600 °C) for 30 min has proven effective at the recrystallization of the $SmCo_5$ hard magnetic phase while keeping α-Fe crystallite sizes in the 10–13 nm range. This also helps to avoid the crystallization of the lower anisotropy Sm_2Co_{17} type hard magnetic phase. The 873 K annealed sample presented a predominant single magnetic phase behavior at 300 K with a value of $\mu_0 H_c$ of 0.39 T and M_r of 90 Am^2/Kg.

Heating the 6 h MM powder to 1323 K, in a thermomagnetic balance, showed the formation of $Sm_2(Co\text{-}Fe)_{17}$ (2 x $SmCo_5$ + 7Fe) alloy as well as an increase of the soft phase crystallite sizes which lead to a two phase type magnetic behavior where the majority of the magnetic domain reversal processes take place around 0 T.

When compared to previous results on $SmCo_5$+30%Fe we notice an increase in $\mu_0 H_c$ and M_r. This increase is due to lowering the annealing temperature below the recrystallization temperature of the Sm_2Co_{17} phase, therefore a larger percentage of the high coercivity $SmCo_5$ is preserved. However, the energy product of the $SmCo_5$+30%Fe samples annealed at 600 °C is significantly lower than that obtained for the $SmCo_5$+20%Fe samples which further reinforces the idea that 30% Fe content is too high, as it results in a 60% drop in coercivity.

In conclusion, we find that annealing on $SmCo_5$+Fe nanocomposite materials should be kept below 873 K, in order to preserve the high anisotropy $SmCo_5$ phase and Fe content should be kept below 30wt%.

Acknowledgments

We acknowledge the financial support from the Romanian Ministry of Research and Innovation, grant PN-III-P1-1.2-PCCDI-2017-0871.

References

[1] J. M. D. Coey, Scripta Mater. **67**, 524 (2012).
[2] R. Skomski, J. M. D. Coey, Scripta Mater. **112**, 3 (2016).
[3] R. Skomski, P. Manchanda, P. K. Kumar, B. Balamurugan, A. Kashyap, D. J. Sellmyer, IEEE T. Magn. **49**, 3215 (2013).
[4] J. M. D. Coey, J. Phys.-Condens. Mat. **26**, 1 (2014).
[5] E. F. Kneller, R. Hawig, IEEE T. Magn. **27**, 3588 (1991).
[6] R. Skomski, J. M. D. Coey, IEEE T. Magn. **29**, 2860 (1993).
[7] L. H. Lewis, D. O. Welch, V. Panchanathan, J. Magn. Magn. Mater. **175**, 275 (1997).
[8] M. Rada, J. Lyubina, A. Gebert, O. Gutfleisch, L. Schultz, J. Magn. Magn. Mater. **290-291 PA**, 1251 (2005).
[9] H. Fukunaga, R. Horikawa, M. Nakano, T. Yanai, T. Fukuzaki, K. Abe, IEEE T. Magn. **49**, 3240 (2013).
[10] Q. Chen, B. M. Ma, B. Lu, M. Q. Huang, D. E. Laughlin. J. Appl. Phys. **85**, 5917 (1999).
[11] J. Zhang, S. Y. Zhang, H. W. Zhang, B. G. Shen, J. Appl. Phys. **89**, 5601 (2001).
[12] D. W. Hu, M. Yue, J. H. Zuo, R. Pan, D. T. Zhang, W. Q. Liu, J. X. Zhang, Z. H. Guo, W. Li., J. Alloy. Compd. **538**, 173 (2012).
[13] S. Tao, Z. Ahmad, P. Zhang, M. Yan, X. Zheng, J. Magn. Magn. Mater. **437**, 62 (2017).
[14] L. Z. Zhao, Q. Zhou, J. S. Zhang, D. L. Jiao, Z. W. Liu, J. M. Greneche, Mater. Des. **117**, 326 (2017).
[15] A. M. Gabay, G. C. Hadjipanayis, M. Marinescu, J. F. Liu, J. Appl. Phys. **107**, 17 (2010).
[16] V. Neu, S. Sawatzki, M. Kopte, Ch. Mickel, L. Schultz, IEEE T. Magn. **48**, 3599 (2012).
[17] J. M. Le Breton, R. Lardé, H. Chiron, V. Pop, D. Givord, O. Isnard, I. Chicinaş, J. Phys. D Appl. Phys. **43**, 085001 (2010).
[18] E. Dorolti, A. V. Trifu, O. Isnard, I. Chicinas, F. Tolea, M. Valeanu, V. Pop, J. Alloy. Compd. **560**, 189 (2013).
[19] V. Pop, E. Dorolti, C. Vaju, E. Gautron, O. Isnard, J. M. Le Breton, I. Chicinaş, Rom. J. Phys. **55**, 127 (2010).
[20] V. Pop, O. Isnard, I. Chicinaş, D. Givord, J. Mag. Magn. Mat. **310**, 2489 (2007).

[21] J. M. D. Coey, Magnetism and Magnetic Materials, Cambridge University Press p. 35 (2010).
[22] H. R. Kirchmayr, H. P. J. Wijn, Landolt-Börnstein – Group III Condensed Matter 19D2- Compounds Between Rare Earth Elements and 3d, 4d or 5d Elements, Springer, p. 327 (1990).
[23] J. J. M. Franse, R. Gersdorf, H. P. J. Wijn, Landolt-Börnstein - Group III Condensed Matter 19a - Condensed Matter 3d, 4d and 5d Elements, Alloys and Compounds, Springer, 144 (1991).
[24] P. Scherrer, Nachr. Ges. Wiss. Goettingen, Math.-Phys. Kl. **1918**, 98 (1918).

*Corresponding author: viorel.pop@phys.ubbcluj.ro